



Covalently bonded multimers of Au₂₅(SBut)₁₈ as a conjugated system

Journal:	<i>Nanoscale</i>
Manuscript ID	NR-ART-03-2018-001902.R2
Article Type:	Paper
Date Submitted by the Author:	29-May-2018
Complete List of Authors:	Sels, Annelies; Universite de Geneve Faculte des Sciences, Département de Chimie Physique salassa, giovanni; University of Geneva, Physical Chemistry Cousin, Fabrice; Laboratoire Léon Brillouin, Lee, Lay-Theng; Laboratoire Léon Brillouin, Bürgi, Thomas; Université de Genève, Department of Physical Chemistry



Journal Name

ARTICLE

Covalently bonded multimers of Au₂₅(SBut)₁₈ as a conjugated system

Received 00th January 20xx,
Accepted 00th January 20xx

Annelies Sels,^a Giovanni Salassa,^a Fabrice Cousin,^b Lay-Theng Lee^b and Thomas Bürgi,^{*a}

DOI: 10.1039/x0xx00000x

www.rsc.org/

Aromatic dithiol linkers were used to prepare aggregates of Au₂₅(SR)₁₈ clusters (SR: thiolate) via ligand exchange reactions. Fractions of different aggregate sizes were separated by size exclusion chromatography (SEC). The aggregates were characterized by UV-vis absorption spectroscopy, matrix assisted laser desorption ionization (MALDI) mass spectrometry, nuclear magnetic resonance (NMR) spectroscopy (including diffusion-ordered spectroscopy, DOSY) and small angle X-ray scattering (SAXS). At 2:1 cluster: dithiol ratio small aggregates were formed (dimers, trimers) but also larger aggregates consisting of 10-20 Au₂₅ clusters, according to DOSY, besides unreacted (monomeric) Au₂₅(SR)₁₈. MALDI mass spectrometry shows signals consistent with dimers and trimers (doubly charged). The SAXS curves for the small aggregates can be well fitted by a pearl-necklace model. For the bigger aggregates the SAXS curves evidence a characteristic separation distance between the clusters within the aggregates, which is imposed by the length of the linker. The SAXS curves of these larger aggregates can be well fitted with a core-shell sphere model with a sticky hard-sphere structure factor, in agreement with closely packed aggregates. The absorption spectra of smaller aggregates resemble the one of individual Au₂₅(SR)₁₈ clusters, however, and most importantly, the larger aggregates show completely different, less structured spectra with a new band emerging at 840 nm. We assign this drastic change of the absorption spectra and the new band to the electronic coupling between the clusters through the all aromatic linker. In accordance with this view, aggregates formed with a linker containing methylene groups, thus breaking conjugation do not show the band at 840 nm. By addition of monothiols to the larger aggregates their size can be reduced through an “unlinking” reaction. This reaction also affects the band at 840 nm, which moves to higher energy when reducing the aggregate size, as would be expected within a particle in a box model. The electronic coupling between the clusters through the linker is the basis for future applications in nanoelectronics.

Introduction

Creating new generations of superstructures by self-assembly of nanosized objects has attracted several research groups for many years due to the great potential applications in molecular electronics or as sensors. A fundamental prerequisite is a highly controlled organization of the particles forming the superstructures.¹⁻³ Gold nanoparticles have been used extensively as building blocks due to their unique high stability and optoelectronic and catalytic properties.^{4,5} A very popular strategy uses DNA covered gold particles, obtaining a highly organized self-assembly.^{6,7} However, heterogeneity in shape and size of the particles affect the particles physicochemical properties and create varying gap sizes after self-assembly.

Monolayer protected gold clusters are optimal building blocks

due to their well-defined structure, high stability and unique size-dependent physical, chemical and optical characteristic.^{8,9} In comparison to gold nanoparticles (NP), thiolate protected gold nanoclusters are atomically precise metal nanostructures.¹⁰ Recent examples have demonstrated that superstructures originated by gold clusters are characterized by unique properties with interesting potential for sensing or other applications.^{11,12}

Formation of superstructures without inducing a structural change of the original cluster could be a challenging task. Ligand exchange reaction is a valuable solution for this problem. It involves the replacement on the Au_n(SR)_m cluster surface of one of the protecting thiol (SR, ligand) with a new entering ligand SR'.¹³ Ligand exchange reaction has been widely studied over the last years and are a known technique that keep the cluster structure intact at least at low thiol concentration.¹⁴ Therefore, the ligand exchange reaction is an extremely useful method to precisely control the number of linking points of the clusters.

Using a bifunctional linker will efficiently connect two clusters together while keeping a defined interparticle distance during assembly.¹⁵ Therefore dithiol ligands which contain two reactive thiol groups can be used in the assembly of the

^a Department of Physical Chemistry, University of Geneva, 30 Quai Ernest-Ansermet, 1211 Geneva 4, Switzerland

^b CEA Saclay, UMR CEA CNRS 12, Lab Leon Brillouin, F-91191 Gif Sur Yvette, France

*Electronic Supplementary Information (ESI) available: All of the UV-Vis, MALDI-TOF and NMR spectra are reported together with every single experiment condition. Detailed SAXS fitting results are provided. See DOI: 10.1039/x0xx00000x

building blocks. Previous work indicated the possibility of intra-cluster exchange using linear alkyl-dithiols.¹⁶ In order to avoid this, rigid linear dithiols are preferred instead. One particular type of linker, aromatic dithiols such as Benzene-1,4-dithiol (**1**) or p-Terphenyl-4,4'-dithiol (**2**) have been used extensively in molecular electronics.¹⁷ The formation of a conducting system will be interesting for the study of energy (or electron) transfer processes.¹⁸

Recently a successful assembly of water-soluble Au₁₀₂(pMBA)₄₀ (where pMBA is *para*-Mercaptobenzoic acid) clusters was achieved via this ligand exchange reactions using diphenyldithiol.¹² Characterization of the isolated species revealed the formation of dimers and trimers, coupled via a disulfide bonding of two exchanged biphenyldithiol. We hypothesize that this disulfide bond will hinder the communication between the linked clusters through the bridge, therefore affecting energy or electron transfer between the clusters and the optical properties of the superstructures.

This study focusses on the connection of Au₂₅(SR)₁₈ clusters by covalently binding the clusters using a bridging agent. To optimize dimer formation and to minimize multimer formation the concentration of dithiols should be kept in deficiency. Via a conducting linker the clusters are expected to communicate, therefore the formation of disulfide bonds is to be avoided. The development of these superstructures could be an important step towards the use of well-defined metal clusters in molecular electronics.

Experimental

Materials: All chemicals were used as received without further purification. Nanopure water (18.2 MΩ) was used in all experiments that involve water. Synthesis of monodisperse Au₂₅(SBut)₁₈ and Au₂₅(PET)₁₈ were performed by following modified protocols.^{19, 20}

Synthesis of clusters: Au₂₅(SBut)₁₈: HAuCl₄•3H₂O (1.0 g) and Tetraoctylammonium bromide (TOABr, 1.575 g) were dissolved in tetrahydrofuran (100 mL). Butanethiol (1.6 mL) was added to the solution and stirred for 1h at room temperature. Next, an aqueous solution of NaBH₄ (0.97 g, 25 mL) at 0 °C was added to the mixture. The orange suspension soon turned into a black-brown solution, indicating the formation of nanoclusters. After 3 days stirring the aqueous phase was removed and the organic phase filtered to remove insoluble residues. This mixture was dried by rotary evaporator and washed with methanol (3 times) to remove free butanethiol and other by-products. The product was dissolved in a minimum amount of toluene and passed over a size exclusion column (SEC). Au₂₅(SBut)₁₈⁻ clusters were separated and confirmed by UV-Vis analysis. Oxidation of the Au₂₅(SBut)₁₈⁻ clusters was performed by passing the cluster over a silica-column (dichloromethane, DCM). Pure Au₂₅(SBut)₁₈⁰ clusters were obtained after washing with MeOH, acetonitrile and extraction with diethylether.

Au₂₅(PET)₁₈: HAuCl₄•3H₂O (1.0 g) and TOABr (1.641 g) were dissolved in tetrahydrofuran (250 mL). PET (1.62 mL) was

added to the solution and stirred for 30 min at room temperature. Next, an aqueous solution of NaBH₄ (0.917 g, 50 mL) at 0 °C was added to the mixture and stirred for 2 days. The washing, purification and oxidation procedure is analogous to the Au₂₅(SBut)₁₈ synthesis.

Dimerization: A stock solution of 2 mg/mL (22.0 mg, 11 mL tetrahydrofuran, THF) Benzene-1,4-dithiol (**1**) was prepared in N₂-atmosphere. 0.05 mL of this solution was added to 10 mg of Au₂₅(SBut)₁₈ clusters, dissolved in 10 mg degassed THF. The reaction was stirred for 24h under constant N₂ atmosphere. The reaction mixture was concentrated to approximately 1 mL and separated over size exclusion chromatography (SX1 bio-beads, Biorad) with THF as eluting agent.

Characterization: Mass spectra were recorded on a Bruker Autoflex mass spectrometer equipped with a nitrogen laser at near-threshold laser intensity in positive linear mode using Trans-2-[3-(4-tert-Butylphenyl)-2-methyl-2-propenylidene] malononitrile (abbreviated as DCTB) as the matrix.

NMR spectra were recorded on Bruker Avance 400 MHz spectrometer. ¹H NMR chemical shifts are given in ppm relative to SiMe₄, with the solvent resonance used as internal reference. Kinetic NMR experiments were performing in a screw-cup NMR tube, dissolving 4 mg Au₂₅(SBut)₁₈ in 0.6 mL of DCM-d₂. The evolution in time of the peak integrals of free thiol were fitted with a three parameters exponential function included in the MestReNova 11.0.1:

$$y = B + F \exp(-x/G)$$

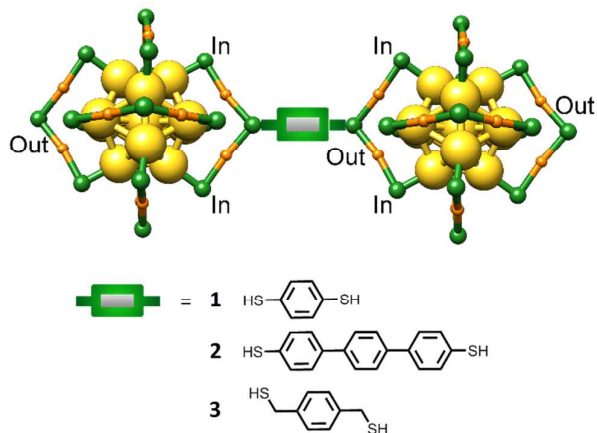
B is the value to which peak integral tends towards at infinite time. We use it to calculate the concentration of free thiols at the equilibrium that, together with the distribution obtain by MALDI spectra, allow obtaining a quantification of all the species at the equilibrium.

Ultraviolet-visible spectra were recorded on a Varian Cary 50 spectrophotometer using a quartz cuvette of 1 cm path length. SAXS experiments were carried out on a Xeuss 2.0 apparatus (Xenocs, France). The instrument uses a microfocused Cu k-alpha source with a wavelength of 1.54 Å and a Pilatus3 detector (Dectris, Switzerland). The experiments were performed with a collimated beam size of 0.5 x 0.6 mm. The sample to detector distance was chosen at 540 mm to achieve a Q range of 0.023 to 0.9 Å⁻¹. The sample solutions were contained in glass capillaries of 1.5 mm external diameter with wall thickness 0.01 mm. Scattering from solvent, empty capillary, and dark field were measured independently and subtracted using standard protocols.²¹ The data were normalized to absolute units. Modelling and fitting were performed with SASVIEW software.

Results and discussion

In order to promote the formation of multimers of Au₂₅(SR)₁₈ (further referred to as Au₂₅) clusters (dimers, trimers and tetramers etc.) rigid dithiol ligands were employed. The characteristics required for the connecting ligands have been: 1) a sufficient separation between the mercapto groups, 2) a rigid structure to avoid intra-cluster binding and 3) π-

conjugated system to facilitate the electronic coupling between the different clusters. Benzene-1,4-dithiol (**1**) and p-terphenyl-4,4''-dithiol (**2**) have shown to possess all these features (Scheme 1). Therefore, ligand exchange reactions between $\text{Au}_{25}(\text{SR})_{18}$ (where SR can be butanethiol "SBut" or 2-phenylethanethiol "PET") and **1** or **2** has been performed using a 2/1 - $[\text{Au}_{25}]/[\text{dithiol}]$ ratio to promote the dimer formation. The reactions have been carried out in N_2 atmosphere to reduce disulfide bond formation. A solution of pure **1** in DCM-d2 was monitored by $^1\text{H-NMR}$, only low amount of disulfide has been observed after 24 h (Figure S1).



Scheme 1. $\text{Au}_{25}(\text{SBut})_{18}$ dimer linked by dithiol ligands 1-3

This has confirmed that the disulfide reaction occurs on a slower time scale than the thiol exchange reaction (leading at the formation of aggregates).

Separation of multimers and UV-Vis/MALDI analysis: Size exclusion chromatography (SEC) is a commonly used and straightforward technique to separate different sizes of clusters.²² Therefore SEC has been used in separating dimers or higher aggregates from monomeric Au_{25} clusters. The crude product of the reaction between $\text{Au}_{25}(\text{SBut})_{18}$ and **1** has been passed over SEC column.

Two bands could be distinguished by eye, however the separation has not been optimal and an intermediate band with mixture of aggregate and pure Au_{25} clusters has been present (Figure S2). The three fractions have been collected, the two major and the middle (transition) fraction, and characterized by UV-Vis and MALDI (Figure 1). UV-Vis spectra (Figure 1A) of the last eluting fraction (**3**, blue trace) has shown the typical features of Au_{25} clusters (Figure S3). The UV-Vis spectra of the second fraction (red trace, corresponding to the transition band in SEC) has appeared similar to the one of Au_{25} . However, the features have been less defined and an additional shoulder at 800-840 nm has emerged. The new signal at 840 nm has also been present in the first eluting fraction (largest structures), where no feature of Au_{25} has been observed. The UV-Vis spectrum of this fraction resembles the one of clusters with size around 2 nm, where neither clear features are observable nor a plasmonic resonance. The UV-Vis changes upon linking reaction have suggested the formation of aggregates (e.g. dimers, trimers, etc.) and the appearance of the absorption band at 840 nm also has indicated a possible electronic coupling between the different Au_{25} units. The possible origin of this feature will be discussed below. MALDI mass spectrometry has been employed to gain more insights on the products formed during the linking reaction. MALDI spectra of the three isolated fractions have been analyzed.

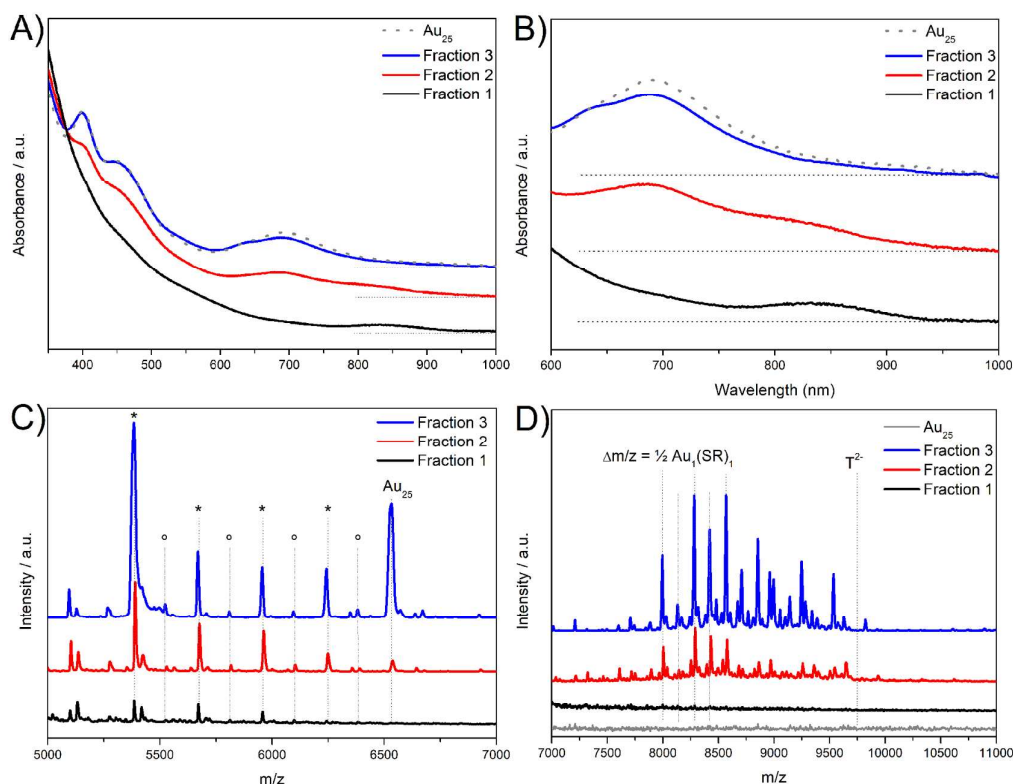


Figure 1: Characterization of separated fractions after size exclusion chromatography by UV-Vis (A) and a zoom of the UV-Vis (B), MALDI in low mass range (C) and high mass range ($m/z > 7000$) (D). Fraction 1 being the first eluting (larger) species and fraction 3 the last eluting species (containing mostly unreacted Au_{25}). Double charged trimers (target m/z : 9756), are indicated (T^2). * indicates loss of $Au(SBu)_1$. ° indicates fragments of double charged species.

Low mass range (Figure 1C) indicates $Au_{25}(SBu)_{18}$ (m/z 6530) is present in the two last eluting fractions (2, red trace and 3, blue trace) but absent in the first sample. The usual fragmentation of Au_{25} clusters, characterized by the loss of a $Au_n(SR)_n$ (*, $n = 1-4$), has been observed. In the mass spectra of all three fractions, this fragmentation pattern is present, however in the first fraction no peak corresponding to Au_{25} has been detected.

This observation suggests that aggregates were present in the sample, which undergo fragmentation similar to parent $Au_{25}(SBu)_{18}$. The presence of more fragments in the MALDI spectra compared to $Au_{25}(SBu)_{18}$ could be explained by the bigger sizes of the aggregates and their minor stability during the MALDI process. Additionally, an unusual fragmentation, corresponding to the loss of $\frac{1}{2} Au_1(SBu)_1$ (°) has been observed. We hypothesize that a double charged species form during MALDI analysis, an effect that is not observed for $Au_{25}(SR)_{18}$. The existence of charged dimers (target m/z : 6510)

is difficult to distinguish from pure Au_{25} clusters and therefore it is difficult to confirm its presence by MALDI. However, looking at higher mass range (Figure 1D: 2, red trace and 3, blue trace), the same fragment separation (distance $\Delta m/z$: $\frac{1}{2} Au_1(SR)_1$) has been detected, which confirms the double charged fragmentation. Note that the onset of the envelope of fragmentation peaks in Figure 1D (2, red trace and 3, blue trace) corresponds well to doubly charged trimers. No defined peak of larger reported clusters (e.g. $Au_{38} = 9625$ or $Au_{40} = 10020$) could be assigned.

We could therefore hypothesize the formation of dimers, trimers and larger aggregates during the linking reaction. As a side note, MALDI of fraction 3 (Figure 1D) displays signals $m/z > 6530$ suggesting presence of dimers/trimers. These are probably resulting from an overlap during separation (SEC). Another important observation is the absence of ligand exchange product $Au_{25}(SBu)_{17}(1)_1$ (m/z : 6581) or higher order. This could raise some doubts about the success of the ligand

exchange reaction. Therefore, NMR spectroscopy has been used to follow the evolution of dithiol **1** during the linking reaction.

NMR analysis: Au₂₅(SBut)₁₈ shows no peaks in the aromatic region of ¹H-NMR spectra. This characteristic has allowed us to follow the evolution of thiol exchange reaction by ¹H-NMR, since no overlap between the signals of cluster and **1** is present. A solution of Au₂₅(SBut)₁₈ and **1** (2/1 ratio between cluster/dithiol) has been prepared in deuterated dichloromethane (DCM-d₂) and the evolution of the signal of the two free thiols (ButSH and **1**) was monitored for 16 h. Figure 2 and Figure S5 show the two signals of **1** (singlets at 3.55 and 7.2 ppm) decreasing until almost disappearing during reaction time. On the other hand, new multiplet signals at 1.3–1.7 ppm and 2.5 ppm which correspond to free butanethiol, appear after 1 h and increase in intensity over time.

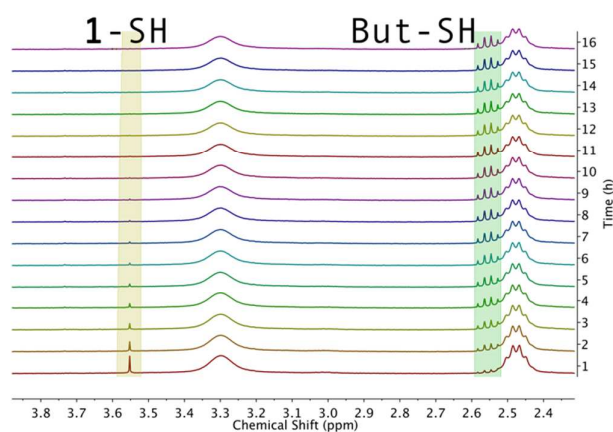


Figure 2: ¹H-NMR (aliphatic region) evolution of thiol exchange reaction between Au₂₅(SBut)₁₈ and **1** (0.5 equiv **1**; 5 mg/mL; DCM-d₂).

Such variation of the NMR peaks has confirmed the exchange of ligands on the surface of Au₂₅. As we recently reported²³ by fitting the evolution of the peak integrals over time it is possible to estimate the percentage of free thiols at the equilibrium. In the case of a 2/1 - Au₂₅(SBut)₁₈/**1** ratio the equilibrium has been reached within around 8 hours and 96% of **1** has been consumed (see Figure S5). Having a closer look at the region of the thiol moiety (3.51–3.77 ppm, Figure S5) we can observe a small peak appearing at 3.74 ppm that we assign to thiol proton of **1** bound to only one Au₂₅. Its intensity increases till 8 hour and decreases afterwards, as expected for an intermediate species. This behaviour suggests that almost all SH groups have reacted, and the thiol exchange reaction has reached completion. The peaks of Au₂₅(SBut)₁₈ (e.g. α_{out} at 5 ppm and β_{in} 3.5 ppm) has undergone broadening due by the loss of symmetry caused by the thiol exchange. Additionally, new broad signal appears around 8.9 ppm (Figure S5), which could originate from the exchanged dithiol.

Therefore, a similar thiol exchange reaction was performed and monitored by ¹H-NMR in which thiophenol, the monothiol variant of **1**, was reacted with Au₂₅(SBut)₁₈. MALDI confirms thiophenol exchanged species which can be the only reason for the NMR signal at 9 ppm. (Figure S6) The recovery of

unreacted Au₂₅ from SEC column (*vide supra*) and the almost complete consumption of **1** indicates that not only dimeric species were formed during the linking reaction but also larger aggregates (multimers). Diffusion-ordered spectroscopy (DOSY) has been a useful tool for size determination of molecules in solution.

Häkkinen and co-worker have reported how DOSY can efficiently determine the hydrodynamic radius of different gold clusters in a nondestructive way.²⁴

We have used the same approach to estimate the size of the aggregates formed after linking reaction. A solution of Au₂₅(SBut)₁₈ and **1** at ratio 2/1 has been reacted overnight and passed through small SEC column (using DCM-d₂) to remove the free thiol present in solution. Figure 3 shows the superimposed DOSY spectra of the cross-linked Au₂₅ and pure Au₂₅(SBut)₁₈. The diffusion coefficient of linked clusters is approximately three times smaller compared to pure Au₂₅(SBut)₁₈ confirming the formation of larger aggregates (see Table 1).

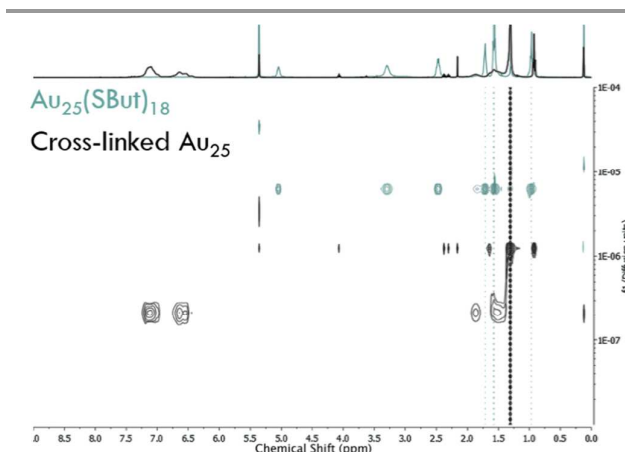


Figure 3: DOSY analysis of cross-linked Au₂₅ – compared to pure Au₂₅ clusters.

As the hydrodynamic radius is inversely proportional to the diffusion coefficient the effective radius of the aggregates is about three times the one of the cluster. Taking the values given in Table 1 the effective volume of the aggregate is about 23 times the one of a single cluster. Considering the void volume between clusters the typical number of linked clusters in an aggregate is smaller than that.

The diffusion coefficient measured with DOSY is the average of all the coefficients of the aggregates that fell under the same NMR peaks. Another important point to consider is that diffusion coefficient calculated from DOSY assumes a spherical model. This of course does not allow one to differentiate all the possible geometries that the aggregate could have after the linking reaction. However from NMR studies we have been able to confirm that the thiol exchange, which is at the base of the linking reaction, is occurring as designed. Furthermore, formation of larger aggregates than dimers has been detected even at low concentration of **1**.

Unlinking reaction: Ligand exchange of thiolate protected gold clusters is a dynamic and reversible reaction. Therefore,

different multimers (e.g. dimers, trimers and larger aggregates) are expected to disassemble after addition of monothiol.

Table 1. Average Diffusion Coefficient and Hydrodynamic Radius of cross-linked Au₂₅ and Au₂₅(SBut)₁₈ in DCM-d2 at 298 K

Au ₂₅ (SBut) ₁₈	Cross-linked Au ₂₅
D = 6.27E ⁻¹⁰ m ² /s r = 0.88 nm	D = 2.13E ⁻¹⁰ m ² /s r = 2.49 nm

Diffusion Coefficient was obtained from the peak at 7.1 ppm. Radius were calculated following Stokes-Einstein equations $r = \frac{k_b T}{6\pi\eta D}$ (parameters are k_b: Boltzman constant; T: 298 K; η(dcm): 0.43 mPa*s)

This unlinking reaction allows us first of all to decrease the size of the aggregates and eventually reform individual Au₂₅ clusters. Second, it should further help us exclude the possibility that the observations described above are due to formation of bigger clusters rather than aggregates of Au₂₅.

An excess of butanethiol (15 equiv) was added to a solution of linked clusters and followed by UV-Vis. Figure 4A shows an increase of characteristic Au₂₅ features after 2h and a decrease of the signal at 840 nm. In a more systematic study the unlinking reaction was followed by UV-Vis with intervals of 20 minutes after addition of a tiny amount of butanethiol (1 equiv). UV-Vis spectra (Figure 4B) show a shift of the peak at 840 nm towards 800 nm with increasing time. After 3h no further change was observed. This could be explained by the presence of free dithiol and free butanethiol in the system at a dynamic equilibrium.

Based on the observations described above we assign the feature at around 840 nm to large conjugated Au₂₅ aggregates. The addition of butanethiol decreases the size of the aggregates and of the conjugated system, resulting in a shift of the band from 840 to 800 nm. Note that the shift of the absorption band around 840 nm towards lower wavelengths and higher energy with decreasing the aggregate size is qualitatively in accordance with a particle in a box model.²⁵ Calculations performed by the Hakkinen group on dimerization of two Au₂₅ clusters through a benzenedithiol predicted no large change in electron density of states.¹⁵

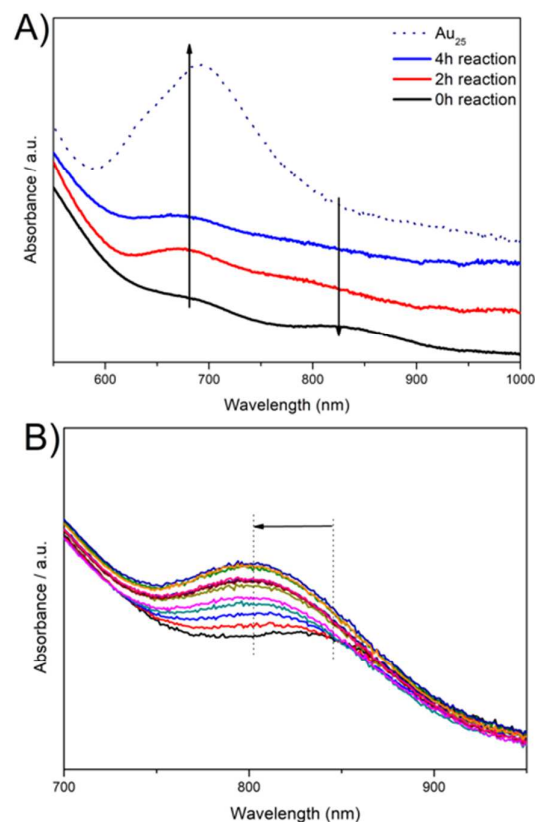


Figure 4: Unlinking reaction of Au₂₅(SBut)₁₈-dimers/trimers with 15 equiv of butanethiol (A) and systematic UV-Vis study (20 min interval) of unlinking reaction with 1 equiv butanethiol (B). Full UV spectra and MALDI after separation in Figure S7.

We therefore think that dimers indeed could have similar UV-Vis absorption spectra as Au₂₅. However formation of larger conjugated systems of Au₂₅ clusters, separated with a defined distance, will change drastically the optical properties.

Throughout our investigation, the largest aggregates of linked clusters precipitated irreversibly after drying. This precipitate was found to be insoluble in any solvent. The formation of large networks of connected clusters, too large to be able to dissolve, could explain this behaviour. Motivated by the unlinking reaction, a large excess of butanethiol was added to a suspension of precipitated Au₂₅(SBut)₁₈-multimers. After 72h the precipitate dissolved and UV-Vis showed again the typical features (800-840 nm) of a multimer solution (Figure S8).

Complementary investigations were performed on the linking reactions between Au₂₅(PET)₁₈ and ligand **1** and **2**. Dithiol **1** was not able to interconnect Au₂₅(PET)₁₈ clusters, the reason for this behaviour lies on the fact that PET is a more hindered ligand than SBut. Therefore, a longer ligand like **2** is needed for the linking reaction to succeed (Figure S9).

Ligand **3** was used to create multimers with formula Au₂₅(SBut)_{18-x}(**3**)_x. In contrast to **1** and **2**, ligand **3** does not allow a direct π-conjugation between the sulfur atoms. This non-conjugate nature affects also the cluster multimers which are not able to electronically communicate. This hypothesis is confirmed by the absence of the band at 840 nm in the UV-Vis spectra of Au₂₅(SBut)_{18-x}(**3**)_x (fraction 1 in Figure S10).

Interestingly, Lahtinen et al have attributed an absorption feature of $\text{Au}_{102}(\text{pMBA})_{40}$ dimers and trimers around 800 nm to a tunnelling charge transfer plasmon effect. Of note, in their system the linking was done via disulfide bond formation, which is expected to break the conjugation. In our case dimers and trimers do not show this band and furthermore larger aggregates linked by the non-conjugated molecule do not present this feature. Therefore, an electronic interaction between the metal clusters and the linker rather than tunnelling seems to be a more plausible explanation in our case.

Additionally the linker length does not seem to influence significantly this feature, which indicates that it is not due to a tunnelling process. Fig S11 shows a comparison between fractions 1 using linker 1, 2 and 3. However, it has to be noted that the multimer fraction is certainly polydisperse, which is also related to the collection of this fraction in the size exclusion chromatography. This polydispersity can be different for the sample with short and long linker, which makes it difficult to spot small differences. Furthermore, we hypothesize that the polydispersity of the multimers induces a broadening of the band at 840 nm, making it furthermore difficult to distinguish small differences between long from short linker. A metal to ligand (MLCT) charge transfer may be at the origin of the absorption band at 840 nm. Further investigations are needed to clarify the nature of this electronic transition.

Small angle X-ray scattering SAXS: Indications of clusters linking by dithiols are presented above. However the size and structure of our multimers remain unknown. Small Angle X-ray Scattering (SAXS) is a powerful tool to measure the size and structure of particles in solution.^{26,27} Since SAXS is based on the scattering length electronic density, the scattering signal originate mainly from the gold (electron-rich) core and staples, scattering signal from the organic protecting shell and the dithiol linker is relatively insignificant. Therefore, the size obtained from these measurements is expected to be smaller than the one derived from a crystal structure of the composite particle. Figure 5 shows the SAXS spectra of pure $\text{Au}_{25}(\text{SBut})_{18}$ clusters compared to a $\text{Au}_{25}(\text{SBut})_{18-x}(\mathbf{1})_x$ sample that is very similar to fraction 2 in UV-Vis/MALDI studies of linked $\text{Au}_{25}(\text{SBut})_{18-x}(\mathbf{1})_x$, which we believed to be in dimeric form. The scattering intensity, normalized by concentration, is plotted as a function of the scattering vector, $Q = 4\pi \sin(\theta) / \lambda$. Qualitatively, the curves show a Guinier plateau corresponding to the finite size of the scattering object, accessible within the Q-range of the measurement. The cut-off of the Guinier plateau occurs at lower Q for the $\text{Au}_{25}(\text{SBut})_{18-x}(\mathbf{1})_x$ confirming its larger size compared to the pure $\text{Au}_{25}(\text{SBut})_{18}$. Secondly, the scattering intensity $I(Q)_{Q \rightarrow 0}$ is proportional to the volume of the scattering object.

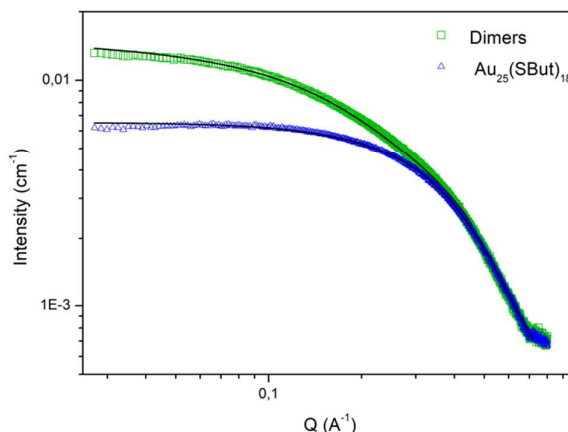


Figure 5: SAXS of pure $\text{Au}_{25}(\text{SBut})_{18}$ clusters and dimers (very similar to the fraction 2 in UV-Vis/MALDI studies) of linked $\text{Au}_{25}(\text{SBut})_{18-x}(\mathbf{1})_x$. The ratio of scattering intensity $I(Q)_{Q \rightarrow 0}$ for $\text{Au}_{25}(\text{SBut})_{18-x}(\mathbf{1})_x$ to $\text{Au}_{25}(\text{SBut})_{18}$ is approximately two.

In this case, $I(Q)_{Q \rightarrow 0}[\text{Au}_{25}(\text{SBut})_{18-x}(\mathbf{1})_x] / I(Q)_{Q \rightarrow 0}[\text{Au}_{25}(\text{SBut})_{18}] \approx 2$, indicating that $\text{Au}_{25}(\text{SBut})_{18-x}(\mathbf{1})_x$ is about twice the volume of pure $\text{Au}_{25}(\text{SBut})_{18}$. A quantitative fit to the $\text{Au}_{25}(\text{SBut})_{18}$ curve using a hardsphere model yields a radius $R \approx 4.6 \text{ \AA}$. On the other hand, the linked sample could not be fitted satisfactorily with a simple hardsphere model. Among models that describe composite structures, we found that a pearl necklace model (hard spheres connected linearly by strings) gives a surprisingly good fit with a dimer structure with particle size $R \approx 5.1 \text{ \AA}$ and particle edge-to-edge distance $L \approx 11.2 \text{ \AA}$. These SAXS results thus give a first indication of dimer linkage using the short linker **1**.

The SAXS spectra for linked clusters for fraction 2 of the UV-Vis/MALDI studies using linker **2**, on clusters with different protecting ligands (PET and SBut) are shown in Figure 6A. A sample of fraction 2 of the UV-Vis/MALDI studies using linker **1** is also shown for comparison. Again, a qualitative analysis based on the ratio of $I(Q)_{Q \rightarrow 0}$ compared to pure Au_{25} cluster gives the relative volumes of the linked clusters. For $\text{Au}_{25}(\text{SBut})_{18}$ (linkers **1** and **2**) the ratio is ~ 2 and for $\text{Au}_{25}(\text{PET})_{18}$ (linker **2**) the ratio is ~ 3 . Based on the previous discussion, these ratios would then indicate presence of dimers and trimers, respectively. Note also that the shoulder is much more pronounced for these samples with linker **2**. This shoulder, a feature related to the linked structure of the particles, occurs at lower Q value for **2** than for **1**, suggesting larger linker distance for **2** (since distance $\sim 1/Q$). These results thus provide further support for the formation of linked structures. A fit with the pearl necklace model yields particle size $R \sim 5 \text{ \AA}$ and particle edge-to-edge distance (related to linker length) $L \sim 20 \text{ \AA}$ for linker **2** and $\sim 11 \text{ \AA}$ for linker **1**. The corresponding scattering curves for fraction 1 of the UV-Vis/MALDI studies are shown in Figure 6B.

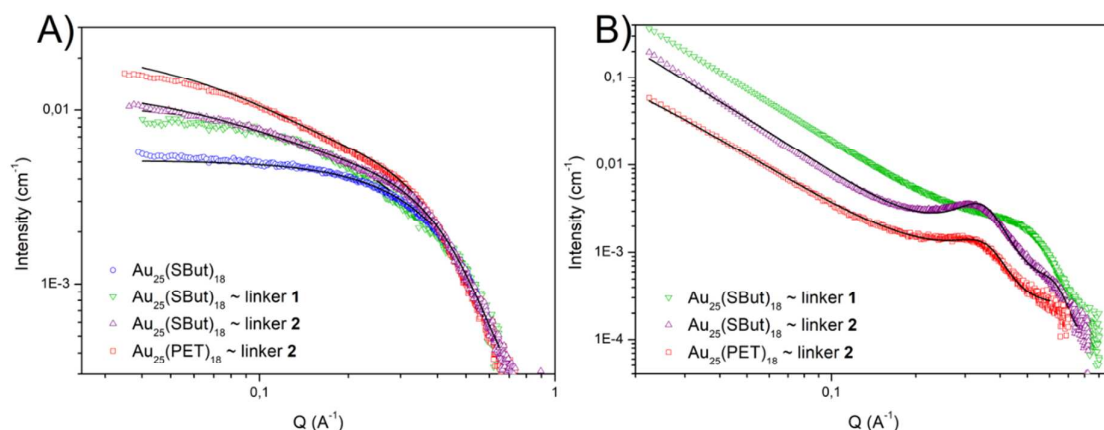
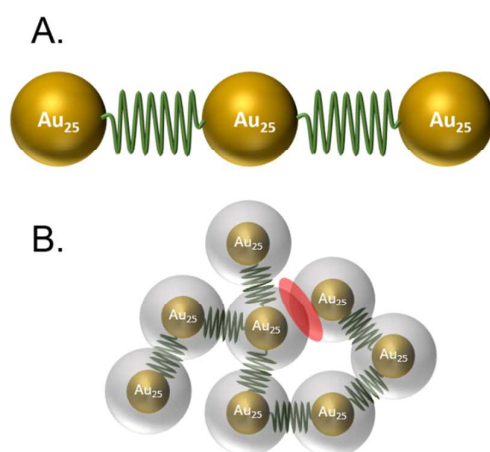


Figure 6: SAXS spectra after SEC for pure $\text{Au}_{25}(\text{SBut})_{18}$ (\bullet), $\text{Au}_{25}(\text{SBut})_{18-x}(1)_x$ (\blacktriangledown), $\text{Au}_{25}(\text{SBut})_{18-x}(2)_x$ (\blacktriangle) and $\text{Au}_{25}(\text{PET})_{18-x}(2)_x$ (\blacksquare). Comparison of fractions 2 (A) of linked clusters and their corresponding fitting, marked in solid line. The ratio of scattering intensity $I(Q)_{Q \rightarrow 0}$ for $\text{Au}_{25}(\text{SBut})_{18-x}(1)_x$ and $\text{Au}_{25}(\text{SBut})_{18-x}(2)_x$ to $\text{Au}_{25}(\text{SBut})_{18}$ is approximately two. The ratio of scattering intensity $I(Q)_{Q \rightarrow 0}$ for $\text{Au}_{25}(\text{PET})_{18-x}(2)_x$ to $\text{Au}_{25}(\text{SBut})_{18}$ is approximately three. Comparison of fractions 1 (B), with the feature of linker 2 at $Q_0 \sim 0.32$ resulting a $d_{c-c} \approx 20$ Å, fitting of the corresponding fractions are marked in solid line. Non-normalized curves can be found in Figure S13

Here, significant small angle rise is observed in all samples, confirming existence of large aggregates. Interestingly, for both ButSH (\blacktriangle) and PET (\blacksquare) - protected clusters using linker 2, the curves also present a clear structure peak indicating the existence of a well-defined characteristic distance within the aggregate structure. From the peak position Q_p , an approximate characteristic distance can be evaluated from the relation $d_{c-c} = 2\pi/Q_p$. For both samples $d_{c-c} \approx 20$ Å.

This is a particle core-to-core distance, and taking into account a particle radius of ~ 5 Å the resulting edge-to-edge distance ~ 10 Å. This distance is smaller than that obtained for dimers and trimers. The reason for this difference might be due to the possible interdigitation of the organic monolayer in between neighbouring clusters (where no rigid dithiol is present).¹⁹ Two interdigitating clusters have shown core-to-core distances to be ~ 13 Å. As represented in Scheme 2B, two types of intercluster distances are possible: the rigid one, established by the linker and the flexible one, arising from random proximity of two clusters (marked in red). The curve for linker 1 shows aggregates but with a less distinct structure peak implying a less organized structure. In an attempt to reproduce the small angle rise due to scattering of the aggregates for linker 2, we have found that a model of core-shell sticky spheres gives a satisfactory fit. Here, the core is made of gold and the shell is constituted of the protective ligands (together with the linker), and the ensemble core-shell particle is attractive. The fitted results give core radius $R \approx 5$ Å and shell thickness $d \approx 5$ Å. These fitted results agree with the d_{c-c} and $d_{\text{edge-edge}}$ evaluated from the position of the structure peak alone, as mentioned above; the model thus reproduces the interparticle organization with a stickiness factor to account for the small angle rise in scattering by the aggregate structure. The results of the fits are given in Table 2.



Scheme 2: Fitting models used in SASVIEW²⁸. (A) the pearl-necklace model and (B) the core-shell sphere model with a sticky hard-sphere structure factor in closely packed aggregates.



Journal Name

ARTICLE

Table 2: (A) Fitted SAXS results of fractions 2 using a pearl necklace model and (B) Fitted SAXS results of fractions 1 using core-shell stickiness sphere model

(A)					(B)		
	Au ₂₅ ●	Sample ■	Sample ▲	Sample ▼		Au ₂₅ (SBut) _{18-x} (2) _x	Au ₂₅ (PET) _{18-x} (2) _x
Cluster	Au ₂₅ (SBut) ₁₈	Au ₂₅ (PET) ₁₈	Au ₂₅ (SBut) ₁₈	Au ₂₅ (SBut) ₁₈	Chi ² /Npts*	144	64
Linker	none	2	2	1	Core radius	4.90 ± 0.11	5.02 ± 0.29
Radius	5.27 ± 0.15	5.08 ± 0.22	5.21 ± 0.16	5.10 ± 0.12	Volfraction	0.12	0.09
Edge					Shell		
Separation		21.2 ± 2.4	19.8 ± 1.2	11.2 ± 2.0	Thickness	5.01 ± 0.55	4.70 ± 0.35
Separation					Perturb	0.01	0.0229 ± 0.001
width		2.36	1.18	1.96	Stickiness	0.098	0.097
N° pearls		3	2	2			

NOTE: Chi² depends on the Q-range of fitting. The values are artificially high due to the poor statistics at high-Q, resulting from solvent effects and low concentrations.

Conclusions

It can be concluded that by addition of dithiols, the structure of the clusters is not affected and this linker can be used to cross-link clusters. A 1:2 ratio of dithiol linker to cluster produced dimers (trimers in the case of PET-protected clusters) as well as aggregates with well-organized internal structures. These species can be fractionated and isolated. The absorption spectra of the large aggregates and unreacted Au₂₅ clusters are drastically different, the former showing a band around 840 nm.

We ascribe this new band to the coupling between the clusters in the aggregates through the linker. DOSY indicates that stable aggregates comprising on the order of 10-20 cluster units are formed. By addition of an excess of monothiols the size of the aggregates can be decreased which shifts the absorption at about 840 nm to higher energies (shorter wavelengths). The obvious coupling between the clusters through the dithiol linkers is of interest in view of applications in optoelectronics or sensing.

Conflicts of interest

There are no conflicts to declare.

Acknowledgements

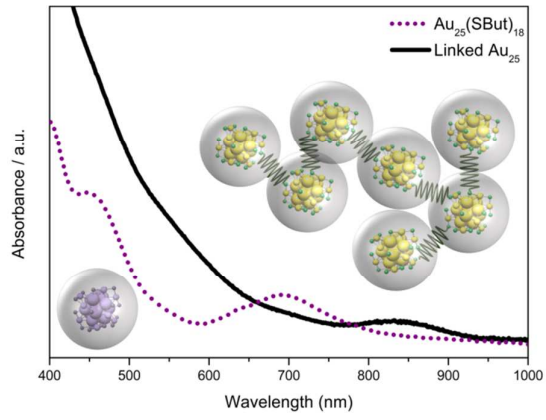
Financial support from the University of Geneva and the Swiss National Science Foundation (grant number 200020_172511) is kindly acknowledged. G.S. thanks EU Horizon 2020 Marie Skłodowska-Curie Action IF GOLDENSENS 747209 for financial support. This work benefited from the use of the SasView application, originally developed under NSF Award DMR-0520547. SasView also contains code developed with funding

from the EU Horizon 2020 programme under the SINE2020 project Grant No 654000.

Notes and references

- N. Hüsken, R. W. Taylor, D. Zigah, J.-C. Taveau, O. Lambert, O. A. Scherman, J. J. Baumberg and A. Kuhn, *Nano Letters*, 2013, **13**, 6016-6022.
- F. Calard, I. H. Wani, A. Hayat, T. Jarrosson, J.-P. Lere-Porte, S. H. M. Jafri, F. Serein-Spirau, K. Leifer and A. Orthaber, *Molecular Systems Design & Engineering*, 2017, **2**, 133-139.
- Z.-Y. Wang, M.-Q. Wang, Y.-L. Li, P. Luo, T.-T. Jia, R.-W. Huang, S.-Q. Zang and T. C. W. Mak, *Journal of the American Chemical Society*, 2018, **140**, 1069-1076.
- A. Fernández-Lodeiro, J. Fernández-Lodeiro, C. Núñez, R. Bastida, J. L. Capelo and C. Lodeiro, *ChemistryOpen*, 2013, **2**, 200-207.
- M. Gadogbe, M. Chen, X. Zhao, S. Saebo, D. J. Beard and D. Zhang, *The Journal of Physical Chemistry C*, 2015, **119**, 6626-6633.
- Y. Zhang, F. Lu, K. G. Yager, D. van der Lelie and O. Gang, *Nat Nano*, 2013, **8**, 865-872.
- F. Sander, U. Fluch, J. P. Hermes and M. Mayor, *Small*, 2014, **10**, 349-359.
- H. Hakkinen, *Nat Chem*, 2012, **4**, 443-455.
- R. Jin, C. Zeng, M. Zhou and Y. Chen, *Chemical Reviews*, 2016, **116**, 10346-10413.
- I. Chakraborty and T. Pradeep, *Chemical Reviews*, 2017, **117**, 8208-8271.
- W. S. Compel, O. A. Wong, X. Chen, C. Yi, R. Geiss, H. Häkkinen, K. L. Knappenberger and C. J. Ackerson, *ACS Nano*, 2015, **9**, 11690-11698.
- T. Lahtinen, E. Hulkko, K. Sokolowska, T.-R. Tero, V. Saarnio, J. Lindgren, M. Pettersson, H. Hakkinen and L. Lehtovaara, *Nanoscale*, 2016, **8**, 18665-18674.
- T. W. Ni, M. A. Tofanelli, B. D. Phillips and C. J. Ackerson, *Inorganic Chemistry*, 2014, **53**, 6500-6502.
- A. Fernando and C. M. Aikens, *The Journal of Physical Chemistry C*, 2015, **119**, 20179-20187.

15. J. Akola, K. A. Kacprzak, O. Lopez-Acevedo, M. Walter, H. Grönbeck and H. Häkkinen, *The Journal of Physical Chemistry C*, 2010, **114**, 15986-15994.
16. V. R. Jupally, R. Kota, E. V. Dornshuld, D. L. Mattern, G. S. Tschumper, D.-e. Jiang and A. Dass, *Journal of the American Chemical Society*, 2011, **133**, 20258-20266.
17. Z. Xie, I. Bâldea, C. E. Smith, Y. Wu and C. D. Frisbie, *ACS Nano*, 2015, **9**, 8022-8036.
18. R. Jin, C. Liu, S. Zhao, A. Das, H. Xing, C. Gayathri, Y. Xing, N. L. Rosi, R. R. Gil and R. Jin, *ACS Nano*, 2015, **9**, 8530-8536.
19. M. De Nardi, S. Antonello, D.-e. Jiang, F. Pan, K. Rissanen, M. Ruzzi, A. Venzo, A. Zoleo and F. Maran, *ACS Nano*, 2014, **8**, 8505-8512.
20. Y. Lu, Y. Jiang, X. Gao and W. Chen, *Chemical Communications*, 2014, **50**, 8464-8467.
21. A. Brulet, D. Lairez, A. Lapp and J.-P. Cotton, *Journal of Applied Crystallography*, 2007, **40**, 165-177.
22. S. Knoppe, J. Boudon, I. Dolamic, A. Dass and T. Bürgi, *Analytical Chemistry*, 2011, **83**, 5056-5061.
23. G. Salassa, A. Sels, F. Mancin and T. Bürgi, *ACS Nano*, 2017, DOI: 10.1021/acsnano.7b06999.
24. K. Salorinne, T. Lahtinen, J. Koivisto, E. Kalenius, M. Nissinen, M. Pettersson and H. Häkkinen, *Analytical Chemistry*, 2013, **85**, 3489-3492.
25. C. Zeng, Y. Chen, K. Iida, K. Nobusada, K. Kirschbaum, K. J. Lambright and R. Jin, *Journal of the American Chemical Society*, 2016, **138**, 3950-3953.
26. A. Baksi, A. Mitra, J. S. Mohanty, H. Lee, G. De and T. Pradeep, *The Journal of Physical Chemistry C*, 2015, **119**, 2148-2157.
27. T. Li, A. J. Senesi and B. Lee, *Chemical Reviews*, 2016, **116**, 11128-11180.
28. M. Doucet, J. H. Cho, G. Alina, J. Bakker, W. Bouwman, P. Butler, K. Campbell, M. Gonzales, R. Heenan, A. Jackson, P. Juhas, S. King, P. Kienzle, J. Krzywon, A. Markvardsen, T. Nielsen, L. O'Driscoll, W. Potrzebowski, R. Ferraz Leal, T. Richter, P. Rozycko, T. Snow and A. Washington, 2017, DOI: 10.5281/zenodo.825675.



Linking of thiolate-protected Au₂₅ clusters by aromatic linker leads to drastic change of optical spectrum